

2003-05-28

Selective Corrosion in Duplex Stainless Steel

Wen-Ta TSAI

Kuen-Ming TSAI

Chang-jian LIN

Yan FU

Recommended Citation

Wen-Ta TSAI, Kuen-Ming TSAI, Chang-jian LIN, Yan FU. Selective Corrosion in Duplex Stainless Steel[J]. *Journal of Electrochemistry*, 2003 , 9(2): 170-176.

DOI: 10.61558/2993-074X.1501

Available at: <https://jelectrochem.xmu.edu.cn/journal/vol9/iss2/8>

This Article is brought to you for free and open access by Journal of Electrochemistry. It has been accepted for inclusion in Journal of Electrochemistry by an authorized editor of Journal of Electrochemistry.

Selective Corrosion in Duplex Stainless Steel

TSAI Wen-Ta^{1*}, TSAI Kuen-Ming¹, LIN Chang-jian^{2*}, FU Yan²

(1. Dept. of Materials Science and Engineering Cheng Kung University Tainan, China,

2. Dept. of Chemistry, State Key Lab. Phgs. Chem. Solid Surfaces,
Xiamen University, Xiamen 361005, China)

Abstract: In duplex stainless steel, the two constituent phases, namely ferritic () and austenitic () phases, have different crystal structure and chemical composition. They may thus exhibit different corrosion resistances in aqueous environment. In this investigation, an electrochemical technique with spatial resolution was employed to measure the potential difference between these two constituent phases in 2205 duplex stainless steel. Image analyzing techniques were also used to examine the preferential corrosion between and phases. The experimental results showed that ferrite had a higher potential than austenite in 0.01 mol/L NaCl solution. In 2 mol/L H₂SO₄ + x mol/L HCl solution, two distinct peaks appeared in the anodic polarization curve in the passive-to-active transition region. Preferential corrosion occurred in the ferrite phase at a lower anodic peak potential, while in austenite at a higher anodic peak potential.

Key words: Duplex stainless steel, Selective corrosion, Micro-area potential distribution

CLC Number: TG 171

Document Code: A

Both the crystal structure and chemical composition of the constituent phases, namely austenitic () and ferritic () phases, in duplex stainless steel (DSS) are different. When exposed in aqueous environment, they may exhibit different electrochemical potentials. Thus, it is expected that selective dissolution will occur due to galvanic coupling within DSS. Yau and Stre-

Received date: 2003-01-11

* To whom correspondence should be addressed, Tel: (86-592)-2189354, E-mail: wttsai@mail.ncku.edu.tw; cjlin@xmu.edu.cn

icher^[1] indicated that selective corrosion of ferritic phase did occur for Fe-Cr-10 % Ni DSS in reducing acid. On the contrary, Sridhar and Kolts^[2] found that austenitic phase in low nitrogen containing DSS corroded preferentially in many different environments. They also found that in high nitrogen containing DSS, selective dissolution occurred in austenitic phase in sulfuric and phosphoric acids while in ferritic phase in hydrochloric acid. Clearly, the nature of the environment which affects the electrochemical potential are also important in deciding the site for selective dissolution in DSS. In the study of dissolution behavior of Fe-21.96 Cr-5.54 Ni-3.04 Mo-0.15N DDS in 2 mol/L H₂SO₄ + 0.1 mol/L HCl and in 2 mol/L H₂SO₄ + 2 mol/L HCl solutions, Symiotis^[3] found that the dissolution rate of ferritic phase was higher than that of the austenitic phase in 2 mol/L H₂SO₄ + 0.1 mol/L HCl solution, but the same in 2 mol/L H₂SO₄ + 2 mol/L HCl solution. Laitinen and Hanninen^[4] pointed out that in 50 % CaCl₂ solution at 100 °C, ferritic phase corroded preferentially in a DSS with a composition of Fe-22.5 Cr-6 Ni-2.85 Mo-0.21N. In acidic (pH = 2) 0.6 mol/L NaCl solution and at passive potential, Schmid-Rieder et al^[5] found that ferritic phase in DSS (Fe-24.4 Cr-6.8 Ni-3.7 Mo-0.21N) was also attacked more easily than austenitic phase. These observations indicated that the constituent phases in a DSS have different susceptibilities to corrosion. Each phase may exhibit an electrochemical potential different from the other, which facilitates the occurrence of galvanic corrosion. The reversion of selective corrosion of the constituent phase may result from the alloying partition in a specific DSS. Furthermore, the susceptibility is also affected by the type or nature of the solution investigated. The potential of each phase in a specific solution, or at least the potential difference between the two adjacent phases are thus of importance in determining the selective dissolution in a DSS.

Therefore, in this investigation, a novel electrochemical technique with spatial resolution was employed to measure the potential of each phase in 0.01 mol/L NaCl solution. The reversion of selective dissolution in a DSS was studied in 5 mol/L H₂SO₄ + *x* mol/L HCl solution. Morphological change associated with selective corrosion was also examined.

1 Experimental

A rod of 2205 duplex stainless steel with a chemical composition (wt %) of Fe-21.95 Cr-5.72 Ni-2.9 Mo-0.174N-0.017C was used. The rod was sliced into several discs each with a thickness of 2 mm for subsequent use. These discs were heat treated either at 1100 °C / 0.5 h or at 1200 °C / 100 h. They were then ground, polished, and etched in Murakami etchant (10 g K₃Fe(CN)₆ + 10 g KOH + 100 mL H₂O) to reveal the duplex microstructure. The respective chemical composition of each constituent phase, namely ferritic and austenitic, was analyzed using energy dispersive spectroscopy (EDS).

The electrochemical potential of each phase in 0.01 mol/L NaCl solution was attempted by employing microprobe technique. The potential difference between ferritic and austenitic was detected. The distribution of surface potential was also monitored using a novel electrochemical technique with

spatial resolution. The investigation on selective dissolution in duplex stainless steel was conducted in 2 mol/L $H_2SO_4 + x$ mol/L HCl ($x = 0.1 \sim 2$) solution under potentiostatic polarization condition. After holding at a predetermined potential for 15 ~ 50 minutes, the surface contour or image was examined by a scanning electron microscope (SEM) or an atomic force microscope (AFM) to reveal the selective corrosion behavior.

2 Results and discussion

Heat treatment could affect the microstructure, grain size, alloying element partition and δ / γ volume ratio in a duplex stainless steel. For the steel heat treated at 1100 / 0.5h, almost equiaxed δ and γ grains were seen with an average grain size of 10 μm . The δ / γ volume ratio was about 40/60. By increasing the heat treatment temperature to 1200 and at a prolonged time (100h), δ phase became the continuous phase and γ grain size was increased to about 70 μm . An example of the optical micrograph of 2205 duplex stainless steel heat treated at 1200 / 100 h is illustrated in Fig. 1.

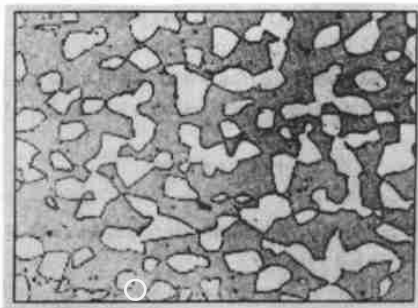


Fig. 1 Micrograph of 2205 duplex stainless steel, annealed at 1200 / 100 h

2.1 Potential Spatial Resolution and Scanning Analysis

A novel microprobe monitoring technique was developed to measure the respective potentials of δ and γ phases of 2205 duplex stainless steel in 0.001 mol/L NaCl solution. The results for the steel heat treated at 1100 / 0.5h are listed in Table 1. With extreme care, either δ or γ of the etched specimen was masked with resin under microscope. The potential of each phase was thus measured using a microelectrode. As shown in Table 1, the potentials of δ and γ were different, with or without masking. The results showed that the ferrite phase had a higher potential than that of austenite. In other words, δ was anodic with respect to γ in 0.01 mol/L NaCl solution.

Tal. 1 Potential differences between austenite and ferrite in duplex stainless steel in 0.01 mol/L NaCl solution(± 10 mV vs. Ag/AgCl)

	Sample	E /mV	No. 1	No. 2
or masked	Ferrite(δ)		161	101
	Austenite(γ)		- 20	28
	Potential difference		181	73
and phases not masked	δ and γ phases		206	256
	Austenite(γ)		- 95	- 28
	Potential difference		301	284

Potential distribution using scanning microprobe technique was also conducted and analyzed. Figure 2 shows the potential variation in an area of $2\,000\ \mu\text{m} \times 2\,000\ \mu\text{m}$. In the examined area, the potential was not constant across the whole area, but scattered in a manner resembling the phase distribution as revealed in the metallograph. The peaks in Fig. 2 might reflect the potential for one phase while the valleys for the other. It is known that, for the 2205 duplex stainless steel, the Cr concentration is lower and N is higher in β phase, in contrast to those of α phase. The difference in alloying element partition was the main cause of the fluctuation of potential measured in 0.01 mol/L NaCl solution.

2.2 Selective Corrosion under Potentiostatic Condition

The potentiodynamic polarization curves of 2205 duplex stainless steel in 2 mol/L $\text{H}_2\text{SO}_4 + x$ mol/L HCl solutions could be affected by the potential scan direction. The curves shown in Fig. 3 were obtained by scanning the potentials from 0 mV (with respect to Ag/AgCl electrode) to the cathodic direction. The results clearly indicated that 2205 duplex stainless steel could be passivated in the solutions investigated though the anodic polarization behavior was strongly affected by the concentration of HCl. The anodic current density increased with increasing HCl concentration. In each anodic curves, there exhibited a passive-to-active transition characteristics. Furthermore, in the transition potential region, two peaks were observed in each anodic curve, which might be associated with two specific reactions. Potentiostatic polarization tests at the peak potentials were thus performed to evaluate the possible reactions involved. The morphological change after potentiostatic polarization was also examined by SEM.

Figures 4 and 5 are the SEM micrographs of 2205 duplex stainless steel after exposing in 2 mol/L $\text{H}_2\text{SO}_4 + 0.5$ mol/L HCl solution and holding at -317 and -263 mV (vs. Ag/AgCl) for 1 800 seconds, respectively. These two potentials were

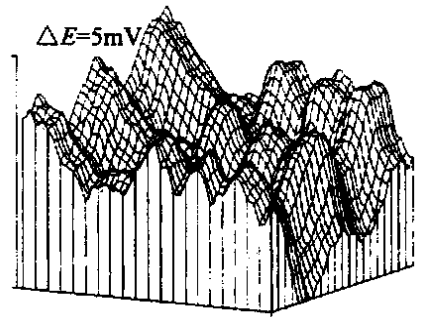


Fig. 2 Potential distribution on surface of 2205 duplex stainless steel in 0.01 mol/L NaCl solution (X and Y axes = $2\,000\ \mu\text{m}$, stepping at 50 and $100\ \mu\text{m}$, respectively), $E = 5\ \text{mV}$

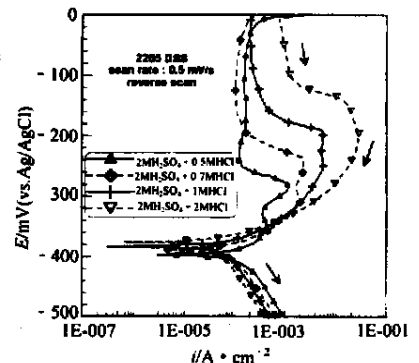


Fig. 3 Potentiodynamic polarization curves of 2205 duplex stainless steel in 2 mol/L $\text{H}_2\text{SO}_4 + x$ mol/L HCl solutions ($x = 0.5 \sim 2$ mol/L), potential scanned from noble to active direction

located at the two peaks as appeared in the polarization curve in Fig. 3 obtained in 2 mol/L H_2SO_4 + 0.5 mol/L HCl solution. At an applied potential of - 317 mV, the SEM micrograph revealed that phase was convex while phase was concave (Fig. 4). The respective phases were identified with EDS. The result indicated that selective corrosion occurred in phase under applied potential at - 317 mV. On the contrary, phase was preferentially attacked and became concave at - 263 mV as depicted in Fig. 5. Though phase corroded at a rate less than that of phase, many pits were found on its surface. The above SEM micrographs not only demonstrated that selective corrosion occurred in 2205 duplex stainless steel, but also indicated that a reversion of selective corrosion could occur if the potential was changed. Similar results were found in 2 mol/L H_2SO_4 solutions with the additions of different concentration of HCl (0.1 ~ 0.2 mol/L).

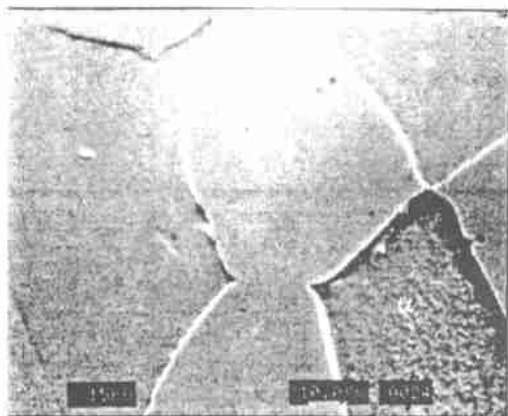


Fig. 4 SEM micrograph showing selective dissolution of phase in 2205 duplex stainless steel in 2 mol/L H_2SO_4 + 0.5 mol/L HCl solution after holding at - 317 mV(Ag/ AgCl) for 1 800 s

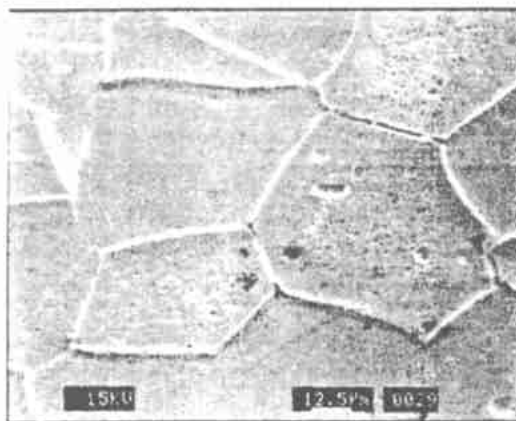


Fig. 5 SEM micrograph showing selective dissolution of phase in 2205 duplex stainless steel in 2 mol/L H_2SO_4 + 0.5 mol/L HCl solution after holding at - 263 mV(Ag/ AgCl) for 1 800 s

AFM was also employed to examine the surface morphology of 2205 duplex stainless steel exhibiting selective corrosion. Fig. 6 shows the AFM image for the specimen immersed in 2 mol/L H_2SO_4 + 0.1 mol/L HCl solution and at - 328 mV for 900 seconds. Clearly, the dissolution rate of phase was higher than that of phase, resulting a significant difference in the surface profile as revealed in Fig. 6.

The occurrence of selective corrosion is no doubt attributed to the partition of alloying elements. Ni and N are enriched in phase while Cr, Mo in phase. It is generally recognized that Cr and N assist passivation of stainless steel. But these two elements are separated in the two different constituent phases. The relative abilities to passivation of these two phases are dependent on the gross composition of duplex stainless steel. In high nitrogen-containing duplex stainless

steel, γ phase may be passivated more easily than α phase because of its higher nitrogen content. The experimental results obtained in this investigation also demonstrated that selective corrosion was greatly affected by the electrochemical potential applied. The results implied that transitions either from active-to-passive or passive-to-active for α and γ phases occurred in different potential regimes. More specifically, the anodic peaks as appeared in Fig. 3 might be dissociated into two curves as shown in the deconvolution diagram of Fig. 7. The deconvolution curves indicate that passive-to-active transition of α phase takes place at a relative lower potential region while it occurs at a relative higher potential region for γ phase. In other words, α and γ phases have different anodic polarization behaviors in the solution investigated. The different surface morphologies as depicted in Fig. 4 and 5 were mainly attributed to the differences in the polarization characteristics of the two constituent phases in the duplex stainless steel.

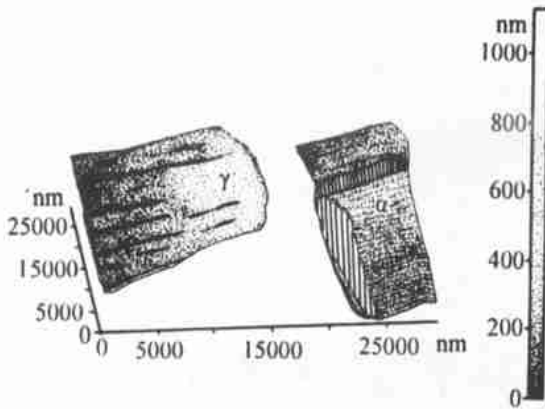


Fig. 6 AFM image showing the difference of dissolution rate between γ / α in 2205 duplex stainless steel in 2 mol/L H_2SO_4 + 0.1 mol/L HCl solution after holding at - 328 mV(Ag/AgCl) for 900 s

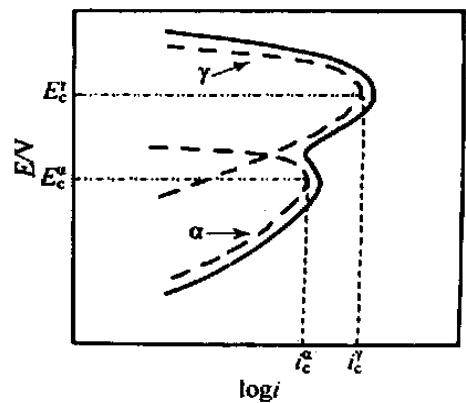


Fig. 7 Schematic diagram showing the deconvolution of the passive-to-active transition in the anodic polarization of 2205 duplex stainless steel in 2 mol/L H_2SO_4 + 0.5 mol/L HCl solution

3 Conclusions

1) An electrochemical technique with special resolution could be used to measure the potential of the constituent phases in 2205 duplex stainless steel. In 0.01 mol/L NaCl solution, the potential for α phases was lower than that γ phases, indicating α was anodic with respect to γ phase.

2) In 2 mol/L H_2SO_4 + x mol/L HCl solution ($x = 0.1 \sim 2$), the potentiodynamic polarization curves exhibited passive-to-active transition characteristics as the potential scanned from anodic to cathodic direction. Two anodic peaks appeared in each anodic polarization curve. Preferential dissolution in duplex stainless steel could occur if the potential was controlled at one of these two peak potentials. A reversion in selective corrosion was observed if the peak potential con-

trolled was reversed.

Acknowledgments

The authors would like to thank the SCC and NNSFC for supporting the work under contract NSC89-2216-E-006-068 and 20127302.

References :

- [1] Yan Y H, Streicher M A. Galvanic corrosion of duplex FeCr-10 %Ni alloys in reducing acids [J]. Corrosion, 1987, 43:366.
- [2] Sridhar N, Kolts J. Effects of nitrogen on the selective dissolution of a duplex stainless steel [J]. Corrosion, 1987, 143:646.
- [3] Symniotis E. Galvanic effects on the active dissolution of duplex Stainless Steels [J]. Corrosion, 1990, 146: 2~12.
- [4] Laitinen A, Hanninen H. Chloride induced stress corrosion cracking of power metallurgy duplex stainless steels [J]. Corrosion, 1996, 52:295.
- [5] Schmidt-Rieder E, Tung X Q, Farr J P G, et al. In situ electrochemical scanning probe microscopy corrosion studies on duplex stainless steel in aqueous NaCl solution [J]. British Corrosion Journal, 1996, 31:139.

双相不锈钢的选择性腐蚀研究

蔡文达^{*1}, 蔡坤铭¹, 林昌健^{2*}, 付 燕²

(1. 台湾成功大学材料与工程学系, 台湾 台南;

2. 厦门大学化学系, 固体表面物理化学国家重点实验室, 福建 厦门, 361005)

摘要: 双相不锈钢中的铁素体(相)和奥氏体(相)具有不同的晶体结构和化学成分,使之在水溶液环境中表现不同的耐蚀特征. 本文应用空间分辨电化学技术测量 2205 双相不锈钢中铁素体和奥氏体的电位差异,并用电镜技术分析了相和相的选择性腐蚀形态. 结果表明,在 0.01 mol/L NaCl 溶液中,铁素体的腐蚀电位比奥氏体高,而在 2 mol/L H₂SO₄ + x mol/L HCl 溶液中,双相不锈钢在活化-钝化电位区出现两个明显的阳极电流峰. 铁素体相的选择性腐蚀发生在较负的阳极峰电位,而奥氏体则在较正的阳极电位峰发生选择性腐蚀.

关键词: 双相不锈钢;选择性腐蚀;微区电位分布